

Supramolecular network formed through O–H...O and π – π stacking interactions: Hydrothermal syntheses and crystal structures of $M(H_2O)_6](optp)_2$ (M = Mg, Ni, Zn, and optp = 1-oxopyridinium-2-thiopropionate)

MURUGAN INDRANI^a, RAMASAMY RAMASUBRAMANIAN^a, FRANK R FRONCZEK^b, DARIO BRAGA^c, N Y VASANTHACHARYA^d and SUDALAIANDI KUMARESAN^{a,*}

^aDepartment of Chemistry, Manonmaniam Sundaranar University, Tirunelveli 627 012

^bDepartment of Chemistry, Louisiana State University, Baton Rouge, LA 70803 1804, USA

^cDipartimento di Chimica G. Ciamician, Univ. of Bologna, Via Selmi 2, 40126 Bologna, Italy

^dSolid State and Structural Chemistry Unit, Indian Institute of Science, Bangalore 560 012

e-mail: skumarmsu@yahoo.com

MS received 14 November 2008; revised 22 May 2009; accepted 12 June 2009

Abstract. A novel class of complexes of the type $[M(H_2O)_6](optp)_2$ (where M = Mg, Ni, Zn, and optp = 1-oxopyridinium-2-thiopropionate) were prepared hydrothermally from metal acetates and 1-oxopyridinium-2-thiopropionic acid (Hoptp), and structurally characterized by X-ray diffraction. Complexes $[Mg(H_2O)_6](optp)_2$ (**1**), $[Ni(H_2O)_6](optp)_2$ (**2**) and $[Zn(H_2O)_6](optp)_2$ (**3**) have isomorphic structures, consisting of one $[M(H_2O)_6]^{2+}$ cation and two anions of Hoptp, which are linked through hydrogen bonding to form extended networks. In each case, the metal cation sits on a crystallographic centre of inversion and binds to six water molecules. The organic anions form a one-dimensional chain with the hexaaquametal(II) moieties via hydrogen bonds.

Keywords. Hydrothermal synthesis; magnesium; nickel; zinc; 1-oxopyridinium-2-thiopropionate; hydrogen bonding.

1. Introduction

We describe here the hydrothermal synthesis of some new inorganic–organic hybrid materials. The increasing interest in hydrothermal synthesis¹ derives from its advantages in terms of high reactivity of reactants, easy control of solution or interface reactions, formation of metastable and unique condensed phases and less air pollution. In addition to the synthesis of new materials, hydrothermal synthesis has been important in biology and environmental sciences, for example, in the origin of life^{2,3} and for decomposing organic wastes.⁴

The self assembly of metal ions with pyridine-*N*-oxide carboxylate groups is a rapidly developing research area of modern coordination chemistry within which ligand design is an important aspect in adjusting the coordination frameworks and functionalities of the products.⁵ To our best knowledge, 1-oxo-

pyridinium-2-thiopropionic acid (Hoptp) has not been much used as a ligand in coordination compounds. This prompted us to undertake a systematic study of Hoptp complexation reactions with alkaline earth metal and transition metals.^{6,7}

The ligand Hoptp possesses several features: (i) it is a polydentate ligand of up to four donor atoms; (ii) the *N*-oxide group has been proved to be more versatile in the coordination mode than pyridine ring because the *N*-oxide's O atom with more lone electron pairs of different orientations provides more flexibility in its coordination geometry than the pyridine's N-atom, which affords straight coordination geometry only; (iii) the steric hindrance is much smaller for *N*-oxide, and in addition, it has the capability of hydrogen bonding; (iv) some *N*-oxides possess important antimicrobial activity;⁸ (v) *N*-oxides are recognized as potential DNA cleaving agents.⁹ Also the pyridine-*N*-oxide derivatives represent a peculiar class of antiviral compounds that qualify as promising novel drugs for exploration as potential

*For correspondence

anti-HIV agents.¹⁰ Transition metal complexes that are suitable for binding and cleaving double-stranded DNA are of considerable current interest due to their chemotherapeutic applications.¹¹ Earlier work has revealed that some drugs show increased activity, when administered as metal complexes rather than as organic compounds.^{12,13}

Using the hydrothermal technique, we have synthesized earlier a series of transition and alkaline earth metal (Co^{2+} , Ni^{2+} , Zn^{2+} and Ba^{2+}) coordination complexes of 1-oxopyridinium-2-thioacetic acid (Hopta) and investigated their crystal structures and the coordination ability of the ligand. The coordination geometry of barium(II) ions in $[\text{Ba}(\mu\text{-opta})_2(\text{H}_2\text{O})_3]_n \cdot 3n\text{H}_2\text{O}$, was described as a distorted dodecahedron,¹⁴ in which the opta anions and a water molecule were forming bridges between two Ba(II) ions whereas in transition metal complexes, the metal ions (cobalt, nickel and zinc) were coordinated only with six water molecules and have distorted octahedral geometry.¹⁵ In this paper, we report the synthesis and structural characterization of simple ionic salt of type $[\text{M}(\text{H}_2\text{O})_6](\text{optp})_2$ with magnesium, nickel and zinc cations.

2. Experimental

2.1 Materials and measurements

The ligand 1-oxopyridinium-2-thiopropionic acid was synthesized as per the reported method.¹⁶ Metal acetates were obtained from Merck (India). All the other chemicals were of analytical grade reagent and used without further purification. Double distilled water was used for preparing all the solutions. IR spectra were recorded on a JASCO FTIR-410 spectrometer using KBr pellets. UV/Vis spectra were recorded on a Perkin Elmer UV/Vis spectrophotometer. Thermogravimetric analysis was performed on a Mettler Toledo Star system with a heating rate of $10^\circ\text{C}/\text{min}$ up to 700°C . Elemental analysis was carried out using a Perkin-Elmer 1400C analyzer.

2.2 Syntheses of $[\text{M}(\text{H}_2\text{O})_6](\text{optp})_2$ ($M = \text{Mg}, \text{Ni}, \text{Zn}$) (1–3)

Complexes **1**, **2**, and **3** were obtained from magnesium(II), nickel and zinc(II) acetate respectively, 1-oxopyridinium-2-thiopropionic acid (Hoptp) and water in the millimolar ratio of 0.125 : 0.250 : 138. The mixtures were homogenized by stirring for 30 min, sealed in a 23 mL polyfluoroethylene-lined

stainless steel bomb. Then the mixtures were heated in a programmable oven at the respective temperatures (100°C for **1**, 130°C for **2**, and 150°C for **3**) and autogenous pressures for the notified time scale (72 h for **1**, 96 h for **2**, and 120 h for **3**). Slow cooling (at $10^\circ\text{C}/\text{h}$) to room temperature produced colourless crystalline blocks for **1** (Yield: 71%), green coloured blocks for **2** (Yield: 75%) and colourless prisms of **3** (Yield: 78%). The crystals obtained (**1**–**3**) were collected by filtration, washed with deionized water followed by diethylether and then air-dried. The preparation of complexes **1**, **2** and **3** is illustrated in scheme 1.

The theoretical contents of C, H and N were calculated for $\text{C}_{16}\text{H}_{28}\text{N}_2\text{O}_{12}\text{S}_2\text{Mg}$ (**1**): C, 36.34; H, 5.34; N, 5.30; S, 12.13%. Analytical results found: C, 36.20; H, 5.20; N, 5.35; S, 12.24%. The theoretical contents of C, H and N were calculated for $\text{C}_{16}\text{H}_{28}\text{N}_2\text{O}_{12}\text{S}_2\text{Ni}$ (**2**): C, 33.12; H, 5.01; N, 4.97; S, 11.38%. Analytical results found: C, 33.03; H, 4.90; N, 5.23; S, 11.47%. The theoretical contents of C, H and N were calculated for $\text{C}_{16}\text{H}_{28}\text{N}_2\text{O}_{12}\text{S}_2\text{Zn}$ (**3**): C, 33.72; H, 4.95; N, 4.92; S, 11.25%. Analytical results found: C, 33.55; H, 4.75; N, 5.25; S, 11.37%.

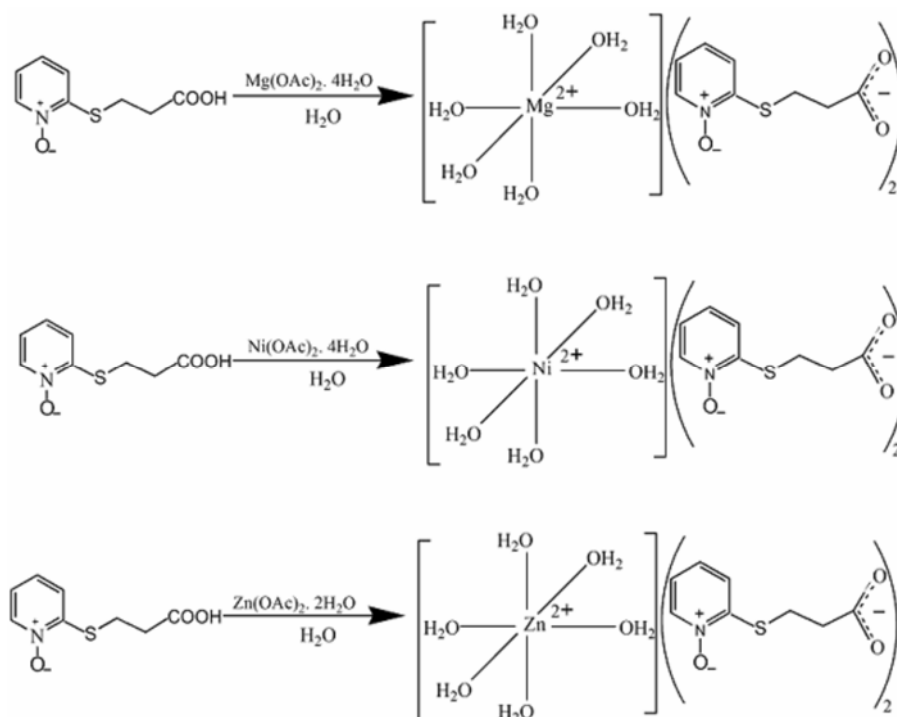
2.3 X-ray data collection

Single crystal of **1** was placed in a cooled nitrogen gas stream at 90 K on a Nonius Kappa CCD diffractometer fitted with an Oxford Cryostream cooler with graphite-monochromated Mo $K\alpha$ radiation. The structure is determined by direct methods and difference-Fourier techniques. SIR97¹⁷ and SHELXL97¹⁸ programs were used to solve and refine the crystal structures.

X-ray diffraction data of **2** were collected at room temperature on a Nonius CAD-4 diffractometer with graphite-monochromated Mo $K\alpha$ radiation. The SHELXL97¹⁸ package was used for structure solution and refinement based on F^2 . All non-H atoms were refined anisotropically.

X-ray data for **3** were collected by graphite-monochromated Mo $K\alpha$ radiation at 298 K. An analytical absorption-correction was applied. The structure was solved by direct methods and refined by full-matrix least-squares with anisotropic temperature factors for non-hydrogen atoms.

All C-bound H atoms in **1**, **2**, and **3** were positioned geometrically (C–H = 0.93–0.97 Å) and refined as riding, with $U_{\text{iso}}(\text{H}) = 1.2U_{\text{eq}}(\text{C})$. The H atoms of water molecules were located in a difference map and refined as riding in their as-found



Scheme 1. Schematic representation of preparation of complexes **1**, **2** and **3**.

relative positions, with $U_{\text{iso}}(\text{H}) = 1.5U_{\text{eq}}(\text{O})$. The software used to prepare the material for publication was PARST97.¹⁹ Crystal data and details of measurements are summarized in table 1.

3. Results and discussion

3.1 Crystal structures

All the $[\text{M}(\text{H}_2\text{O})_6](\text{optp})_2$ complexes are isostructural and crystallize in triclinic space group $P\bar{1}$. The metal ion is located at an inversion center and octahedrally coordinated by six aqua ligands, which is associated with two 1-oxopyridinium-2-thiopropionate ions through hydrogen bond interactions. The optp organic anions form a one-dimensional chain with the $[\text{M}(\text{H}_2\text{O})_6]^{2+}$ moieties, mediated by hydrogen bonds. Thus, the organic component serves both as a charge balancing counter ion and a chemical entity that participates in extensive hydrogen bonding. Stable $[\text{M}(\text{H}_2\text{O})_6]^{2+}$ octahedral cations in several Co(II), Ni(II), and Zn(II)^{20,21} systems have been reported. In this work, deviation of the coordination geometry from ideal octahedral coordination seems to be an essential requirement to form hydrogen bonds between coordinated water molecules and the organic moiety.²²

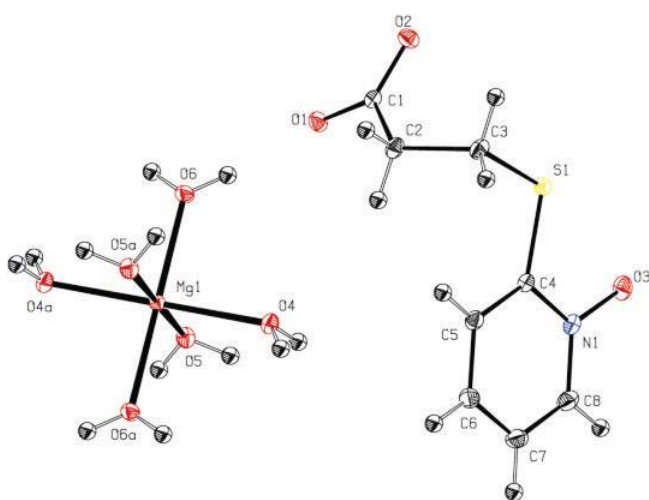
An ORTEP diagram of **1** is shown in figure 1. Selected bond lengths and bond angles of **1–3** are

given in table 2. The M–O distances are 2.1093(6)–2.0562(6) Å for **1**, 2.084(4)–2.035(2) Å for **2**, and 2.141(2)–2.056(2) Å for **3**, respectively. These values agree well with the reported M–O distances in similar water octahedral systems.^{23,24} The N–O bond distances (1.3318(8)–1.326(2) Å) of optp are found to be elongated compared to the average N–O value (1.30(2) Å) of a typical non-coordinated *N*-oxide.²⁵ The bond lengths of C(1)–O(1) and C(1)–O(2) are 1.2653(8) and 1.2613(9) Å for **1**, 1.255(4) and 1.250(3) Å for **2**, and 1.249(2) and 1.257(2) Å for **3**, which are in agreement with the reported values.²²

The O(3)–N(1)–C(4)–S(1) moiety of optp is found to be a part of a regular heterocyclic hexagon. The N(1)–C(4)–S(1) bond angles [112.84(5)–113.02(16)°] show a significant distortion from the expected value of 120° towards the pyridine-*N*-oxide O atom,²⁶ which indicate that the S atom is bent considerably towards the O atom of *N*-oxide. In all the three structures N(1)–C(8) distance (1.3590(4) Å; for **1**) of optp is slightly shorter than that of N(1)–C(4) (1.3662(9) Å; for **1**), while the average N–C bond length in the pyridine ring is 1.36(2) Å. Complexes **1**, **2**, and **3** display intermolecular H-bonding interactions (figure 2 and tables 3–5). Complexes **1**, **2**, and **3** have both O–H...O and C–H...O types of interactions. In **1**, each cationic

Table 1. Crystal data and structure refinement for **1**, **2** and **3**.

Complex	1	2	3
Empirical formula	MgC ₁₆ H ₂₈ N ₂ O ₁₂ S ₂	NiC ₁₆ H ₂₈ N ₂ O ₁₂ S ₂	ZnC ₁₆ H ₂₈ N ₂ O ₁₂ S ₂
Formula weight	528.83	563.23	569.90
Temperature (K)	90(2)	293(2)	293(2)
Wavelength (Å)	0.71073	0.71073	0.71073
Crystal system	Triclinic	Triclinic	Triclinic
Space group	P $\bar{1}$	P $\bar{1}$	P $\bar{1}$
Unit cell dimensions			
<i>a</i> (Å)	7.1242(10)	7.14(2)	7.174(5)
<i>b</i> (Å)	7.5528(11)	7.499(3)	7.525(5)
<i>c</i> (Å)	11.752(2)	11.682(4)	11.737(5)
Volume (Å ³)	573.31(15)	568.6(17)	575.6(6)
<i>Z</i>	1	1	1
<i>D</i> _{calc} (Mgm ⁻³)	1.532	1.645	1.644
Absorption coefficient (mm ⁻¹)	0.324	1.102	1.312
<i>F</i> (000)	278	294	296
Crystal size (mm)	0.28 × 0.25 × 0.17	0.27 × 0.24 × 0.17	0.41 × 0.24 × 0.18
θ Range for data collection (°)	2.88–40.25	3.05–24.97	1.87–25.40
Limiting indices	–12 ≤ <i>h</i> ≤ 12 –13 ≤ <i>k</i> ≤ 13 –21 ≤ <i>l</i> ≤ 21	–8 ≤ <i>h</i> ≤ 8 –8 ≤ <i>k</i> ≤ 8 0 ≤ <i>l</i> ≤ 13	–8 ≤ <i>h</i> ≤ 8 –9 ≤ <i>k</i> ≤ 9 –14 ≤ <i>l</i> ≤ 14
Reflections collected/unique	21246/7141	1992/1992	4777/2118
<i>R</i> _{int}	0.0222	0.0000	0.0289
Completeness to θ (%)	99.8	99.8	99.7
Absorption correction	None	None	Analytical
Refinement method	Full-matrix least-squares on <i>F</i> ²	Full-matrix least-squares on <i>F</i> ²	Full-matrix least-squares on <i>F</i> ²
Data/restraints/parameters	7141/0/171	1992/0/176	2118/6/170
Goodness-of-fit on <i>F</i> ²	1.050	1.116	1.003
<i>R</i> ₁ and <i>wR</i> ₂ [<i>I</i> > 2σ(<i>I</i>)]	0.0345 and 0.090	0.0275 and 0.0790	0.0250 and 0.0678
<i>R</i> ₁ and <i>wR</i> ₂ (all data)	0.0427 and 0.0939	0.0284 and 0.0796	0.0264 and 0.0685
Largest difference peak and hole (eÅ ⁻³)	0.601 and –0.695	0.343 and –0.435	0.242 and –0.377

**Figure 1.** An ORTEP diagram of **1** with atomic numbering. Thermal ellipsoids are drawn at 40% probability level.

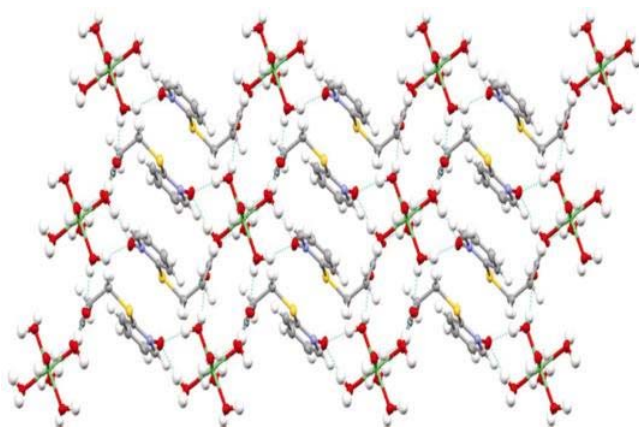
unit connects eight anionic moieties through O–H...O interactions. The corresponding five O–H...O interactions [O(4)–H(4A)...O(3), O(5)–H(5A)...O(3), O(6)–H(6A)...O(1), O(6)–H(6B)...O(1) and O(4)–H(4B)...O(2)] collectively construct corrugated one-dimensional ribbons along *c*-direction in [101] plane. These ribbons are constituted by alternate pairs of R₂² (8) and R₂¹ (6) rings. The anions are positioned in such a way that they adopt opposite orientation in alternating ribbons. The adjacent ribbons are interlinked by O(5)–H(5B)...O(2) [*d*_{O(5)–H(5B)...O(2)} (*x* – 1, *y* – 1, *z*) = 2.7233(8) Å and \angle = 171.5(14)°] interactions which make the one-dimensional ribbons into a two-dimensional array in [101] plane. Similar interactions are also observed in complexes **2** and **3**.

The packing diagram of [M(H₂O)₆](optp)₂ with hydrogen bonds viewed along *a*-axis appears like a sheet. When viewed along *c*-axis, it resembles

Table 2. Selected bond lengths (Å) and angles (°) for **1**, **2** and **3**.

Compound 1			
Bond lengths (Å)			
Mg(1)–O(4)	2.0832(6)	N(1)–O(3)	1.3318(8)
Mg(1)–O(5)	2.1093(6)	C(1)–O(1)	1.2653(8)
Mg(1)–O(6)	2.0562(6)	C(1)–O(2)	1.2613(9)
Bond angles (°)			
O(6)–Mg(1)–O(5) ⁱ	90.13(2)	O(4)–Mg(1)–O(5)	88.69(2)
O(4)–Mg(1)–O(6) ⁱ	89.27(2)	O(5)–Mg(1)–O(4) ⁱ	91.31(2)
O(6)–Mg(1)–O(4)	90.73(2)	O(2)–C(1)–O(1)	124.14(6)
O(6)–Mg(1)–O(5)	89.87(2)		
Compound 2			
Bond lengths (Å)			
Ni(1)–O(4)	2.084(4)	N(1)–O(3)	1.326(2)
Ni(1)–O(6)	2.065(3)	C(1)–O(1)	1.255(4)
Ni(1)–O(5)	2.0352(17)	C(1)–O(2)	1.250(3)
Bond angles (°)			
O(1)–C(1)–O(2)	124.31(19)	O(4)–Ni(1)–O(5) ⁱⁱ	90.25(8)
O(5)–Ni(1)–O(4)	89.75(8)	O(6)–Ni(1)–O(4)	90.07(18)
O(5)–Ni(1)–O(6)	90.26(8)	O(4)–Ni(1)–O(6) ⁱⁱ	89.93(18)
O(6)–Ni(1)–O(5) ⁱⁱ	89.74(8)	O(5)–Ni(1)–O(4) ⁱⁱ	90.25(8)
Compound 3			
Bond lengths (Å)			
Zn(1)–O(4)	2.0993(15)	N(1)–O(3)	1.332(2)
Zn(1)–O(5)	2.1405(16)	C(1)–O(1)	1.249(2)
Zn(1)–O(6)	2.0563(19)	C(1)–O(2)	1.257(2)
Bond angles (°)			
O(4)–Zn(1)–O(6) ⁱ	90.52(5)	O(5)–Zn(1)–O(4) ⁱ	89.44(7)
O(6)–Zn(1)–O(5) ⁱ	89.79(6)	O(4)–Zn(1)–O(5)	90.56(7)
O(6)–Zn(1)–O(5)	90.21(6)	O(1)–C(1)–O(2)	123.93(16)
O(6)–Zn(1)–O(4)	89.48(5)		

Symmetry transformations used to generate equivalent atoms: (i) $-x + 1, -y + 1, -z + 1$;
(ii) $-x, -y, -z$

**Figure 2.** A perspective view of 3-D supramolecular network of **1**.

an infinite ladder (figure 3),²⁷ with the ‘uprights’ defined by the anionic optp units and the ‘steps’ by the extended $M(H_2O)_6^{2+}$ arrays. In between two steps in the ladder there arises a rhombic grid made with O(6) and O(6)ⁱ atoms of water [symmetry code: (i) $-x + 1, -y + 1, -z + 1$] and O(1) atom of optp, and this hydrogen bonded motif is notated as $R_2^2(8)$.²⁸

The cationic units, $Mg(H_2O)_6^{2+}$ are bridged by the carboxylate oxygen atoms [O(1)] by O(6)–H(6A)···O(1) and O(6)–H(6B)···O(1) hydrogen bonds which build one-dimensional chains constituted by $R_4^2(8)$ rings along *b*-direction in *bc*-plane. These chains along with the corrugated one-dimensional ribbons form a 3-D framework. The

Table 3. Hydrogen bonds in **1**

D–H...A	D–H (Å)	H...A (Å)	D...A (Å)	D–H...A (°)
O(4)–H(4A)...O(3) ⁱ	0.862(15)	1.899(15)	2.7386(9)	164.1(14)
O(4)–H(4B)...O(2) ⁱⁱ	0.842(15)	1.868(15)	2.7066(8)	173.7(15)
O(5)–H(5A)...O(3) ⁱ	0.848(15)	1.908(15)	2.7446(9)	168.5(14)
O(5)–H(5B)...O(2) ⁱⁱⁱ	0.832(15)	1.898(15)	2.7233(8)	171.5(14)
O(6)–H(6A)...O(1)	0.841(15)	1.906(15)	2.7419(8)	172.6(15)
O(6)–H(6B)...O(1) ^{iv}	0.863(17)	1.861(17)	2.7177(8)	171.4(16)

Symmetry codes: (i) $-x + 1, -y + 1, -z$; (ii) $x, y - 1, z$; (iii) $x - 1, y - 1, z$; (iv) $1 - x, 2 - y, 1 - z$

Table 4. Hydrogen bonds in **2**.

D–H...A	D–H (Å)	H...A (Å)	D...A (Å)	D–H...A (°)
O(4)–H(4B)...O(3)	0.94(4)	1.83(4)	2.742(3)	166(3)
O(4)–H(4A)...O(2) ⁱ	0.66(3)	2.12(3)	2.755(6)	163(4)
O(6)–H(6A)...O(3) ⁱⁱ	0.85(4)	1.89(4)	2.738(4)	172(3)
O(6)–H(6B)...O(2) ⁱⁱⁱ	0.88(3)	1.83(3)	2.705(4)	173(4)
O(5)–H(5A)...O(1) ^{iv}	0.85(4)	1.85(4)	2.696(4)	174(3)
O(5)–H(5B)...O(1) ^v	0.81(3)	1.96(3)	2.757(3)	169(3)

Symmetry codes: (i) $1 - x, 1 - y, 1 - z$; (ii) $-x, -y, -z$; (iii) $x, y - 1, z - 1$; (iv) $-x, 1 - y, 1 - z$; (v) $x, y, z - 1$

Table 5. Hydrogen bonds in **3**.

D–H...A	D–H (Å)	H...A (Å)	D...A (Å)	D–H...A (°)
O(4)–H(4A)...O(3) ⁱ	0.828(10)	1.923(11)	2.738(2)	168(2)
O(4)–H(4B)...O(1) ⁱⁱ	0.837(9)	1.871(10)	2.705(2)	175(2)
O(5)–H(5A)...O(1) ⁱⁱⁱ	0.844(10)	1.926(12)	2.755(2)	167(2)
O(5)–H(5B)...O(3) ^{iv}	0.844(10)	1.925(12)	2.750(2)	165(2)
O(6)–H(6A)...O(2) ^v	0.835(10)	1.930(11)	2.750(2)	167(2)
O(6)–H(6B)...O(2) ⁱⁱ	0.848(10)	1.849(11)	2.693(2)	173(2)

Symmetry codes: (i) $-x + 1, -y + 1, 2 - z$; (ii) $x, y + 1, z$; (iii) $-x, -y, 1 - z$; (iv) $x, y, z - 1$; (v) $1 - x, 1 - y, 1 - z$

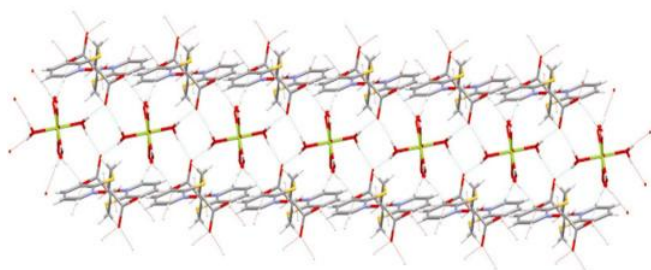


Figure 3. Projection of the structure of **1** viewed along reciprocal c -axis.

pyridine rings in a given layer are all parallel. The layers are held together by O–H...O hydrogen bonds involving the carboxylate group, N–O moiety and the coordinated water molecules. The most impor-

tant structural feature of **1** is the extensive network of hydrogen bonds, which not only connects the optp⁻ anions to the magnesium complex, but also relates the adjacent anions through the O atoms of carboxylate and the *N*-oxide group. Because of the parallel arrangement of the optp anions of neighbouring units, there exists a π – π stacking interaction of 3.668 Å (figure 4) between the pyridine rings. Both hydrogen-bonding and π – π interactions combine to stabilize the three-dimensional supramolecular network.

3.2 Infrared spectra of complexes **1–3**

The free Hoptp molecule exhibits IR absorption bands at 833 and 1094 cm⁻¹ for N–O bending and stretching vibrations, respectively. Nevertheless, a

considerable change in N–O bending vibrations at 823 cm^{-1} in the complexes indicate the involvement of hydrogen bonding. The broad and intense band at 3236 cm^{-1} is due to O–H stretching vibrations of water. The bands at 1561 and 1421 cm^{-1} are due to the anti-symmetric and symmetric stretching vibrations of carboxylate group. The bands at 1466 and 1421 cm^{-1} are characteristic of C=C and/or C–N bonds of the pyridine *N*-oxide ring. The C–H out-of-plane bending vibrations of the pyridyl ring appear at 765 and 742 cm^{-1} . The band at 707 cm^{-1} indicates the C–S stretching vibration. The weak bands below 600 cm^{-1} are attributed to the $\nu(\text{MO})$ vibrations.²⁹

3.3 Thermogravimetric analysis for 1–3

Thermogravimetric analysis (TGA) of **1**, **2** and **3** were carried out under an inert atmosphere of dry nitrogen. The TGA curve of **1** exhibits three stages of weight losses. The first weight loss is 19.5% (calculated 20.4%) in the temperature range of 88–125°C, corresponding to the loss of six coordinated water molecules. The second weight loss of 38.2% (calculated 37.63%) in 230–290°C is ascribed to the release of one optp. The third stage reveals further decomposition, leading to the formation of oxide of magnesium.

The TGA curve of **2** exhibits three steps of weight losses. The first stage of the decomposition (100–120°C) corresponds to the loss of six-coordinated water molecules (calculated 19.1%; found 20.4%). The second stage of decomposition leads to the loss of one optp (250–260°C). The final stage involves

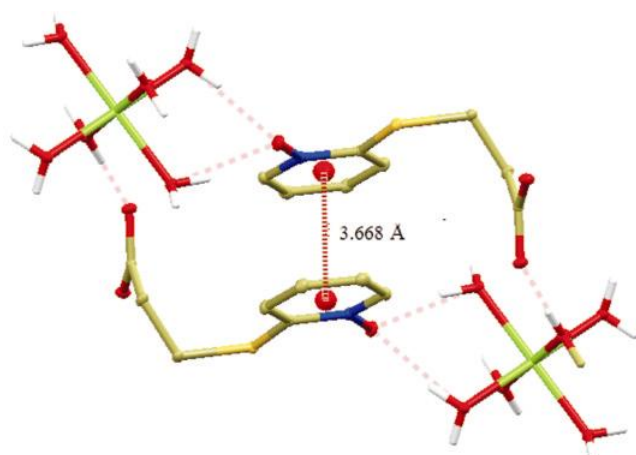


Figure 4. π – π interactions in $[\text{Mg}(\text{H}_2\text{O})_6](\text{optp})_2$ (**1**).

the further decomposition and leads to the formation of oxides and/or sulphides of nickel. The TGA curve of **3** exhibits similar weight loss stages to those of **2** (See supplementary information figure S1).

3.4 Electronic spectra

The UV-Vis spectra of all complexes show absorption bands at 330 nm, which may be assigned to the π – π^* transitions of optp. In addition, the nickel complex shows two absorption bands at 400 and 700 nm, which are attributed to the d – d transitions of the metal ions.³⁰ See supplementary information figure S2.

3.5 Magnetic susceptibility measurement of 2

Variable-temperature magnetic susceptibility data of **2** were measured in 10–300 K. The effective magnetic moment is $3.2\ \mu_{\text{B}}$, which is close to the value of $3.9\ \mu_{\text{B}}$ expected for the isolated high-spin Ni(II). A χ_{M} versus T plot (figure 5), in which χ_{M} is the corrected magnetic susceptibility per Ni(II) unit, can be fitted to the Curie–Weiss law $\chi_{\text{M}} = C/(T - \theta)$, giving a Curie constant $C = 1.28\text{ cm}^3\text{ mol}^{-1}\text{ K}$, and a Weiss constant $\theta = -14.19\text{ K}$. Small negative value of Weiss constant (θ) shows a weak intermolecular anti-ferromagnetic interaction between nickel ions, probably via hydrogen bonds. The χ_{M} value of $4.19 \times 10^{-3}\text{ cm}^3\text{ mol}^{-1}$ at room temperature increases as the temperature decreases, attaining a value of $5.4 \times 10^{-2}\text{ cm}^3\text{ mol}^{-1}$ at 10 K.

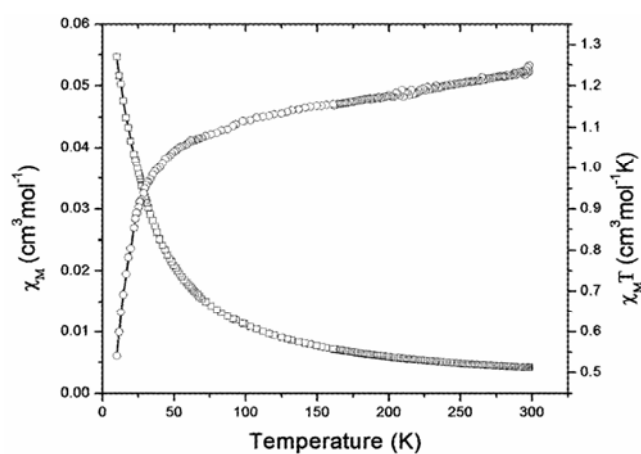


Figure 5. Temperature dependence of χ_{M} and $\chi_{\text{M}}T$ for complex **2**.

4. Conclusion

In summary, three new complexes, hexaaquamagnesium(II) 1-oxopyridinium-2-thiopropionate, hexaaquanickel(II) 1-oxopyridinium-2-thiopropionate, and hexaaquazinc(II) 1-oxopyridinium-2-thiopropionate were synthesized by hydrothermal reactions and their structures were characterized by X-ray crystallography, IR, UV/Vis spectra, elemental analysis and magnetic susceptibility measurements. Small negative value of Weiss constant (θ) shows a weak intermolecular antiferromagnetic interaction in **2**.

Acknowledgements

The authors (MI and RR) acknowledge Council of Scientific and Industrial Research (CSIR), New Delhi for providing financial support through Senior Research Fellowship. FRF acknowledges the purchase of the diffractometer by Grant No. LESQSF (1999–2000)-ENH-TR-13, administered by the Louisiana Board Regents.

Supplementary data

CCDC No. 672466, 672467 and 672468 contain the supplementary crystallographic data for [Mg(H₂O)₆](optp)₂ (**1**), [Ni(H₂O)₆](optp)₂ (**2**), and [Zn(H₂O)₆](optp)₂ (**3**). These data can be obtained free of charge via <http://www.ccdc.cam.ac.uk/conts/retrieving.html>, or from the Cambridge Crystallographic Data centre, 12 Union road, Cambridge CB2 1EZ, UK; fax: (+44) 1223-336-033; or e-mail: deposit@ccdc.cam.ac.uk. Supplementary figures S1 and S2 can be found in website (www.ias.ernet.in/chemsci).

References

- Feng S and Xu R 2001 *Acc. Chem. Res.* **34** 239
- Baross J A and Deming J W 1983 *Nature* **303** 423
- Jannasch H W and Mottle M J 1985 *Science* **229** 717
- Yesodharan S 2002 *Curr. Sci.* **82** 1112
- Landers A E and Phillips D J 1981 *Inorg. Chim. Acta* **51** 109
- Indrani M, Ramasubramanian R, Kumaresan S, Hu M-L and Soriano-García M 2008 *Acta Cryst.* **C64** m23
- Indrani M, Ramasubramanian R, Kumaresan S and Soriano-García M 2007 *Anal. Sci.* **23** x127
- Danish I A and Rajendraprasad K J 2003 *Acta Pharm.* **53** 287
- Ganley B, Chowdhury G, Bhansali J, Scott Daniels J and Gates K S 2001 *Bioorg. Med. Chem.* **9** 2395
- Balzarini J, Stevens M, Clercq E D, Schols D and Pannecouque C 2005 *J. Antimicrobial Chemotherapy* **55** 135
- Sigman D S, Mazumdar A and Perrin D M 1993 *Chem. Rev.* **93** 2295
- Hodnett E M and Mooney P D 1970 *J. Med. Chem.* **13** 786
- Hodnett E M and Dunn W J 1972 *J. Med. Chem.* **15** 339
- Ramasubramanian R, Kumaresan S, Indrani M, David Stephen A, Kumaradhas P, Thomas R and Awen B Z 2007 *Anal. Sci.* **23** x149
- Kumaresan S, Ramadevi P, Walsh R, McAneny A and Lake C H 2006 *J. Chem. Sci.* **118** 243
- Ramasubramanian R, Kumaresan S, Thomas R, Stephen A D and Kumaradhas P 2007 *Cryst. Res. Technol.* **42** 1024
- Altomare A, Burla M C, Camalli M C, Cascarano G L, Giacovazzo G L, Guagliardi A, Moliterni A G G, Polidori G and Spagna R 1999 *J. Appl. Cryst.* **32** 115
- Sheldrick G M 1997 SHELXL97 University of Göttingen, Germany
- Nardelli M 1995 *J. Appl. Cryst.* **28** 659
- Knutti P 1981 *Inorg. Chim. Acta* **52** 141
- Carriati F, Erre L, Micera G, Panzanelli A, Ciani G and Sironi A 1983 *Inorg. Chim. Acta* **80** 57
- Benedetti E, Bavoso A, Blasio B, Pavone V and Pedone C 1986 *Inorg. Chim. Acta* **123** 155
- Otterson T, Warner L G and Seff K 1974 *Acta Cryst.* **B30** 1188
- Ray S, Zalkin A and Templeton D H 1973 *Acta Cryst.* **B29** 2741
- Chao M H, Kumaresan S, Wen Y S, Lin S C, Hwu J R and Lu K L 2000 *Organometallics* **19** 714
- Hartung J, Svoboda I and Fuess H 1996 *Acta Cryst.* **C52** 2841
- Vivar M E D, Baggio S, Garland M T and Baggio R 2007 *Acta Cryst.* **C63** m123
- Etter M C and Mac Donald J 1990 *Acta Cryst.* **B46** 256
- Nakamoto K 1997 *Infrared and Raman spectra of inorganic and coordination compounds* (New York: Wiley) 3rd edn
- Lever A B P 1968 *Inorganic electronic spectroscopy* (New York: Elsevier) 2nd edn